Effect of Precipitation pH and Heat Treatment on the Properties of Hydrous Zirconium Dioxide

Article *in* Russian Journal of Inorganic Chemistry · March 2008

DOI: 10.1134/S0036023608030029

ISSN 0036-0236, Russian Journal of Inorganic Chemistry, 2008, Vol. 53, No. 3, pp. 350–356. © Pleiades Publishing, Ltd., 2008.
Original Russian Text © I.A. Stenina, E.Yu. Voropaeva, A.G. Veresov, G.I. Kapustin, A.B. Yaroslavtsev, 2008, published in Zhurnal Neorganicheskoi Khimii, 2008, Vol. 53, No. 3, pp. 397–403.

SYNTHESIS AND PROPERTIES OF INORGANIC COMPOUNDS

Effect of Precipitation pH and Heat Treatment on the Properties of Hydrous Zirconium Dioxide

I. A. Stenina[a], E. Yu. Voropaeva[a], A. G. Veresov[b], G. I. Kapustin[c], and A. B. Yaroslavtsev[a]

[a] *Kurnakov Institute of General and Inorganic Chemistry, Russian Academy of Sciences, Leninskii pr. 31, Moscow, 119991 Russia*

[b] *Chemistry Department, Moscow State University, Vorob'evy gory, Moscow, 119992 Russia*

[c] *Zelinsky Institute of Organic Chemistry, Russian Academy of Sciences, Leninskii pr. 47, Moscow, 119991 Russia*

Received March 30, 2007

Abstract—The effect of the precipitation pH and subsequent heat treatment is studied on the properties of hydrous zirconium dioxide precipitated by ammonia from nitrate solutions. Precipitation at pH ≤ 6 generates hydrous zirconium dioxide, which contains excess sorbate nitrate ions; the product precipitated at pH ≥ 7 contains excess ammonium ions. This distinction considerably affects the course of thermolysis and the morphology of products. The exotherm associated with the formation of the crystal structure of zirconia becomes more pronounced with rising precipitation pH. In addition, the samples prepared at pH ≥ 7 have a more developed surface. The morphologic and microstructural evolution of hydrous zirconium dioxide samples during thermolysis is described.

DOI: 10.1134/S0036023608030029

Zirconium dioxide is one of the most popular subject of study in materials science. Its popularity is primarily due to its chemical and thermal stability as well as to the unique conducting and sorptive properties of materials based on it. The precursor for zirconium dioxide is, as a rule, hydrous zirconium dioxide. The synthesis and thermolysis of this compound are abundantly documented. The methods used to prepare hydrous zirconia oxide include sol–gel technology, electrochemical synthesis, hydrothermal treatment, and others [1–5]. However, precipitation with alkalis from solutions of zirconium salts is used far more frequently.

Hydrous zirconium dioxide is a globular hydrate [6, 7]. The core of a nanosized particle of such materials is, as a rule, composed of oxides or hydrous oxides. Their surface bears many hydroxide groups, which balance the coordinative unsaturation of surface atoms. OH groups, depending on the nature of the element to which they are bound, can dissociate as an acid or base and, accordingly, participate in cation or anion exchange reactions [5–7]. In addition, such particles adsorb water molecules, which provide for the high proton mobility both on the surface and in the bulk of the material [8, 9].

The surface properties of hydrous zirconium dioxide considerably change during heat treatment [4, 5, 8]. The specific surface area [4] and ionic conductivity [8] of this material pass through a well-defined maximum during thermolysis. Another factor influencing the surface properties of hydrous zirconium dioxide is the precipitation pH. For example, it was shown in [9] that composite materials prepared from hydrous zirconium dioxide precipitated at various pHs considerably differ in their properties. Presumably, this is because of the adsorption of various types of cations or anions during synthesis [10], these species considerably affecting the agglomeration ability of the material.

This work studies the evolution during thermolysis of hydrous zirconium dioxide samples that were precipitated with ammonia from nitrate solutions at various pHs.

EXPERIMENTAL

Hydrous zirconium dioxide was precipitated with concentrated aqueous ammonium hydroxide from a 0.2 M solution of zirconium oxynitrate (pure grade, from Vekton) at various pHs (3 ≤ pH ≤ 10). Two sets of samples were prepared. The samples of set I were centrifuged after precipitation and, then, exposed in Petri dishes at –12°C in a refrigerator; after thawing out, precipitates were decanted and dried in air for 2 days at room temperature. The samples of set II were washed six times with large amounts of water by means of decantation and with centrifugation. Then, precipitates were exposed in Petri dishes at –12°C in a refrigerator; after thawing out, they were again washed with large amounts of water, centrifuged, and dried in air at room temperature for 2 days.

Physicochemical methods were used to characterize test samples. X-ray powder diffraction was carried out on a D/MAX-2000 Rigaku diffractometer (Cu$K_{\alpha 1}$ radi-

ation). The coherence length was calculated from the Debye–Scherrer relationship

$$d = 0.9\lambda/(\beta\cos\theta), \quad (1)$$

where λ is the X-ray length, equal to 1.54178 Å; β is the physical line broadening; and θ is the line position. For the monoclinic phase, the average width of (-111) and (111) reflections was chosen. Sodium chloride was the reference.

Electron diffraction patterns were recorded in the general diffraction mode on a BR-100 transmission electron microscope.

Microstructure was examined using a Supra 50 VP LEO scanning electron microscope.

Potentiometric titration was carried out with an Econix-Expert pH meter with Mettler-Toledo combination pH electrodes. The pH value was automatically recorded every 3 s. Equilibrium pH after addition of every aliquot of a sodium hydroxide solution was found by extrapolation of pHs to infinite experimental time τ, which corresponded to $1/\tau = 0$.

Thermal analysis was carried out on a TG 209 F1 Iris Netzsch thermobalance in platinum crucibles followed by the analysis of leaving gases on an Aeolos QMS 403 C Netzsch mass spectrometer. The heating rate was 5 K/min; sample sizes, 50–55 mg; and temperature range, 25–900°C. For selected samples, differential thermal analysis was simulated using the instrument software.

Specific surface areas were determined on a volumetric setup as in [11].

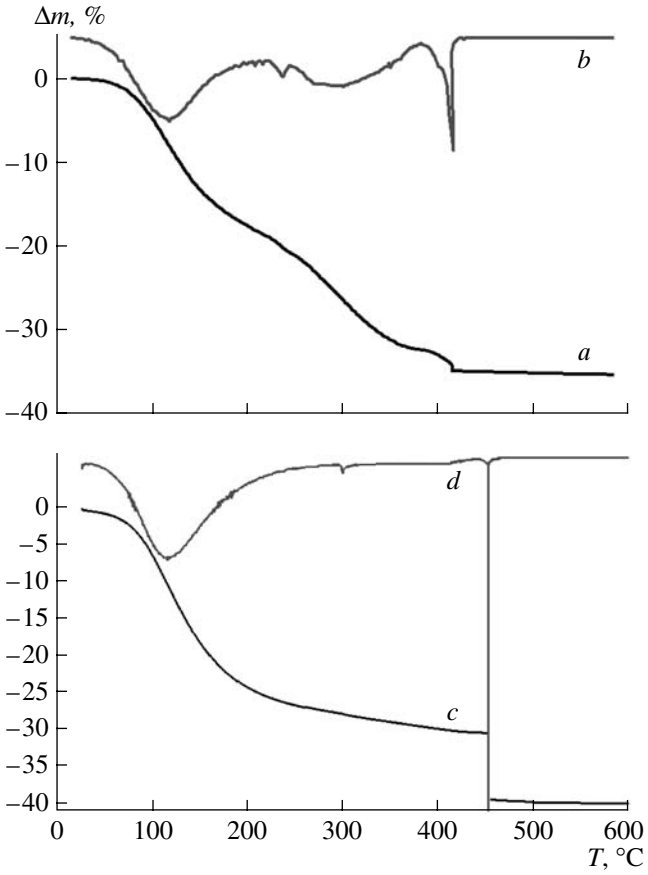

Fig. 1. (*a*, *c*) Weight-loss curves and (*b*, *d*) differential weight-loss curves for hydrous zirconium dioxide samples prepared at pH equal to (*a*, *b*) 4 and (*c*, *d*) 10.

RESULTS AND DISCUSSION

Proceeding from their thermal curves, the test samples can be categorized into two groups: A and B. For each group (Fig. 1), samples decomposed in several stages. For the IA and IIA group samples (Figs. 1*a*, 1*b*), which were prepared at pH ≤6, loss of weakly bound water (which is retained on the surface due to weak hydrogen and coordination bonds) is observed at low temperatures (below 230–250°C) (Figs. 1a, 2a), and a far weaker peak is due to removal of molecules with the mass number (M/z) equal to 44 (Fig. 2a). To this mass number, carbon dioxide or nitrous oxide can correspond. Almost for all samples the curve of elimination of molecules with $M/z = 44$ is identical to the curve for molecules with $M/z = 12$, which has a far lower intensity. From this, we can infer that the curve for molecules with $M/z = 44$ describes carbon dioxide evolution. The overall weight loss at the first stage reaches 18–22%; then, a narrow weight-loss peak is observed with a peak temperature of 250–275°C, which is associated with the elimination of molecules with the same mass number (44). The relevant DTA feature is an exotherm (a peak with heat evolution). Proceeding from the small width of the peak and its exothermicity, we can conclude that it is associated with a phase transition. In the range 260–380°C, there is another broad peak. The substances lost at this stage are ammonia ($M/z = 15$), nitrogen oxides ($M/z = 30$ (NO) and 46 (NO_2)), carbon dioxide, and a small amount of water. The overall weight loss for IA set samples reaches 31–33%. At 420–450°C, another narrow peak is recorded with a far greater intensity than the peak at 250–275°C. For the samples prepared at low pHs, the weight loss is not great and is determined by the evolution of ammonia and nitrogen oxides (NO and NO_2). The relevant DTA feature is an exotherm, also associated with a phase transition. For the samples prepared at high pHs, this effect is so intensive that resembles a microexplosion and is accompanied with dispersion. It cannot be ruled out that the decomposition of ammonium nitrate, which is pyrophoric because of decomposition to nitrous oxide and water, is involved. This agrees with the fact that the gas-evolution peak with $M/z = 44$ has the higher intensity than the peak with $M/z = 12$. After this, the weight loss almost ceases, and another 2–3 wt % is only lost in the range 750–800°C. None of the most likely decomposition products was detected. This peak corresponds to $M/z = 19$ and is due to the evolution of fluorine, which is an impurity to zirconium oxynitrate.

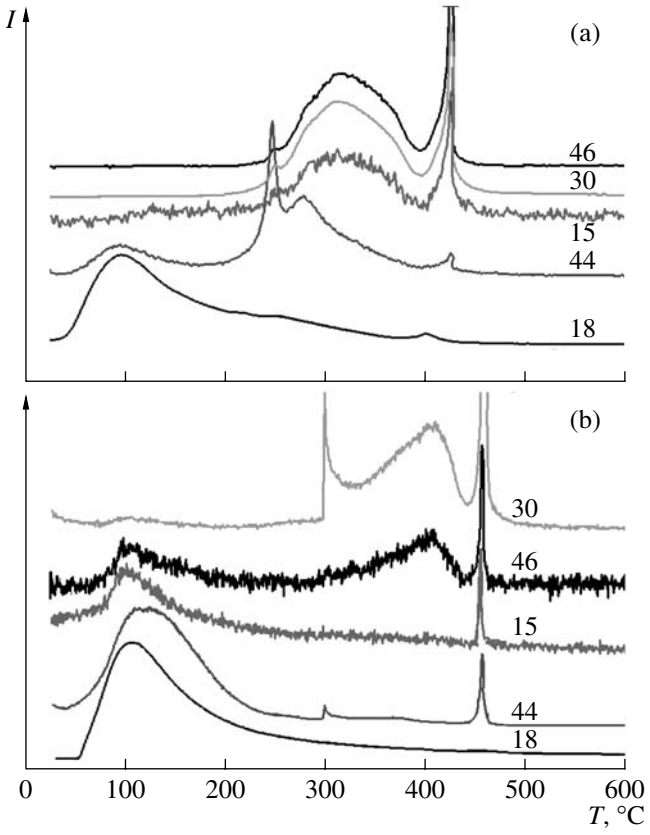

Fig. 2. Gas-flow intensities for hydrous zirconium dioxide samples prepared at pH equal to (a) 4 and (b) 10. The figures above the curves indicate the mass numbers (M/z) for the relevant ions.

An increase in the number of washing cycles for the set IIA samples results in an increase in weight loss at the first stage (25–230°C) to 22–24%. At subsequent stages, weight loss considerably decreases with an attendant decrease in the evolution of nitrogen oxides and ammonia. The intensities of the relevant peaks weaken. Thus, at $T > 200$°C, some amount of nitrate ions and ammonia is remained sorbed on the surface or in the bulk of the sample. This casts doubt on the high concentration of surface OH groups on a monoclinic ZrO_2 sample found in [5] by means of thermal analysis. The concentration of surface OH groups was determined in [5] to be 20.2 μmol/m^2, corresponding to the occurrence of hydroxide groups at all zirconium atoms and the protonation of all surface oxygen atoms. The increase in the OH group concentration after the acid or alkali treatment of zirconium dioxide is also doubtful [5]. According to our data, only additional adsorption of anions or cations occurs, increasing the weight loss upon heating. The carbon dioxide evolution line (M/z = 44) changes even more greatly. At the first thermolysis stage (25–230°C), the carbon dioxide evolution increases noticeably, while the fraction of firmly anchored CO_2 (which is lost at 420–450°C) decreases considerably. This is likely because the concentration of weakly bound (physisorbed) carbon dioxide decreases with time of water treatment.

For the set IB samples precipitated at pH ≥ 7 (Figs. 1*c*, 1*d*), thermolysis differs from that for set IA samples. The weight loss at the first low-temperature stage slightly increases to reach 22–27% (Fig. 1c). The desorption of ammonia and nitrogen oxides (in smaller amounts than in the preceding case) occurs simultaneously with dehydration (Fig. 2b). The temperatures of all stages rise substantially. The temperature of the first weight-loss spike increases to 307–320°C; that of the second one increases to 460°C. The peak temperatures clearly tend to rise with increasing precipitation pH. The overall intensity of the ammonia flow rises, whereas the overall intensity of the nitrogen oxide flow decreases. The weight loss in the range 200–400°C decreases considerably. The greatest changes are observed in the region of the second exotherm: the weight loss at this stage increases to 2–5% and becomes a well-defined jump (Figs. 1*c,* 1*d*). The analysis of an sample of expelled gases indicates that they mainly consist of nitrogen oxides (M/z = 30, 44, and 46) and ammonia. It cannot be ruled out that the weight loss at this stage is considerably contributed by the desorption of carbon dioxide, which is absorbed from the atmosphere during the precipitation and washing of the sample because of the existence of an alkaline medium. However, the stronger weight change and heat evolution, as well as the occurrence of both nitrogen oxides and ammonia in the vapor, imply that the rapid desorption of nitrate ions and ammonia at elevated temperatures cause them to react on the zirconia surface and induces intense heat evolution. This implication is verified by a considerable decrease in the weight jump and heat evolution with increasing number of washing cycles.

The samples of set IIB precipitated at pH ≥ 7 have the same distinctive features as those of set IIA, i.e., the decreased amounts of nitrogen oxides and ammonia evolved. At the same time, the temperatures of all transformations for the set II samples are virtually independent of pH; they are only subject to insignificant probabilistic fluctuations (±10 K). For comparison, for the IA set samples (which experienced fewer washing cycles), the exotherm temperatures increase by 40–70°C as the precipitation pH changes from 4 to 10.

Hydrous zirconium dioxide is a good ion-exchange material, with cation-exchange properties dominating at high pHs and anion-exchange properties dominating at low pHs [12]. The equivalence point for the adsorption of sodium and chloride ions is close to 6.5. From these data, we can infer that hydrous zirconium dioxide containing mostly adsorbate anions (NO_3^-) is formed at pH ≤ 6. A small amount of ammonia is adsorbed as counterions. At pH ≥ 7, ammonium ions should be mostly adsorbed. According to thermal analysis, how-

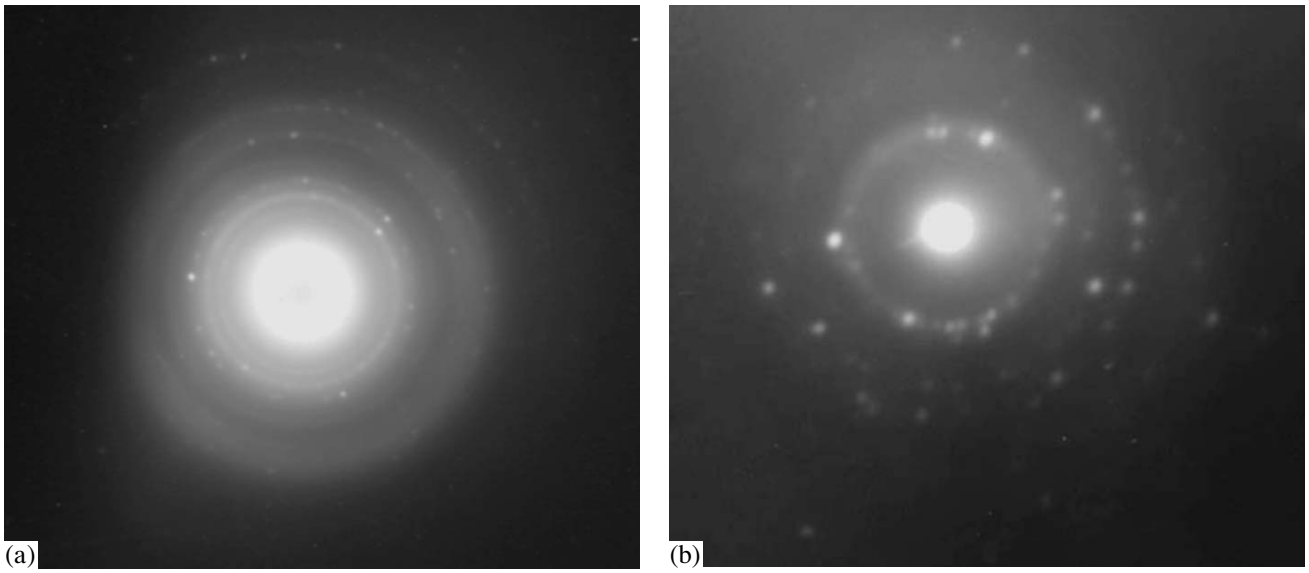

Fig. 3. Electron diffraction patterns for a hydrous zirconium dioxide sample prepared at pH 7 (a) without heat treatment and (b) after treatment at 300°C.

ever, the sample also contains considerable amounts of nitrate ions. Even careful washing does not fully remove these ions. According to [10], the nitrate ion concentration in solution during precipitation, e.g., at pH 6, is about seven orders of magnitude that of hydroxide ions. Accordingly, the surface of the sample with well-defined ion-exchange properties adsorbs NO_3^- ions from solution and transforms to the substituted form. In the weakly alkaline region (pH 7–9), in contrast, ammonium ions substitute for the hydrogen ions of –Zr–OH groups. Nitrate ions, whose concentration is 10^4 to 10^6 times that of hydroxide ions, are simultaneously occluded from solution during the formation of sparingly soluble hydrous zirconium dioxide.

Potentiometric titration data verify this suggestion. The precipitation of hydrous zirconium dioxide occurs fairly smoothly, without kinks in the pH versus amount of base curve. This means that OH– ion-exchange groups with various surroundings and dissociation constants are formed in a globule. Ion exchange proceeds over the entire range of pH values; it can involve either the substitution of NO_3^- anions for OH groups in the acidic region or the substitution of cations (Na^+) for OH^- groups in the alkaline region. The ion-exchange capacities for both substitution scenarios are comparable; the equivalence point is observed at pH $\approx$ 7, in agreement with data in [12]. From the data obtained, we can infer that the hydrous zirconium dioxide samples precipitated at pH $\leq$ 6 mostly contain sorbate nitrate anions and those precipitated at pH $\geq$ 7 mostly contain sorbate ammonium ions. It is for this reason that the oxides precipitated from solutions in the acidic and alkaline regions have considerably differing properties.

As expected, hydrous zirconium dioxide samples are X-ray amorphous at room temperature. However, their electron diffraction patterns show several weak reflections (Fig. 3a), which indicate the appearance of a certain structure inside globules; this structure cannot be classified as any known phase of zirconium dioxide or zirconium hydroxide. Temperature elevation to 350°C likewise does not induce crystallization, as shown by X-ray powder diffraction. Electron diffraction, a more sensitive technique, shows that the globule matrix becomes crystalline after the first exotherm (Fig. 3b).

A well-defined structure of monoclinic ZrO_2 is observed starting at 400°C (Fig. 4). Crystallization is accompanied by the expulsion of foreign species from the matrix of globules, namely, ammonium, nitrate, and hydrogen ions, which inhibit the formation of the zirconium dioxide crystal structure. The particle size of the monoclinic phase (the coherence length) increases as the sample is heated from 400 to 500°C, then decreasing. The minimum coherence lengths are observed for the samples calcined at 600–700°C (Fig. 5), because the formation of crystalline zirconia finishes at these temperatures, and insignificant, remnant gas evolution results in the destruction of crystals. Subsequently, the crystal size again increases because of rising diffusion mobility.

The specific surface areas measured for test samples are listed in the table. After samples prepared at low pHs were calcined at 100°C, their specific surface areas remain rather low, being equal to 1–2 m^2/g. For samples prepared at pH $\geq$ 7, the surface area approaches 200 m^2/g. This signifies a considerable effect of the

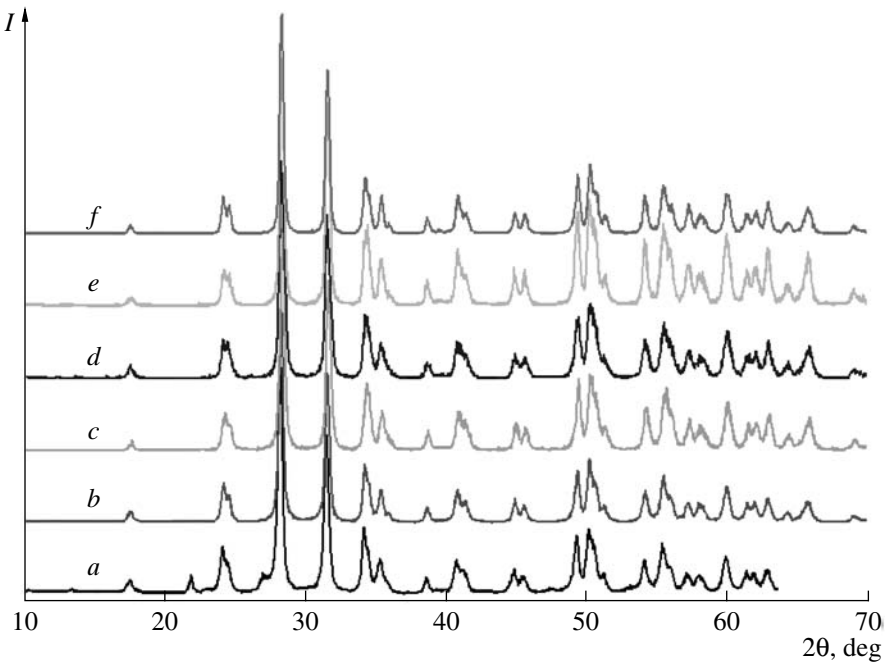

Fig. 4. X-ray diffraction patterns for a hydrous zirconium dioxide sample prepared at pH 9 after calcining to (a) 400°C, (b) 500°C, (c) 600°C, (d) 700°C, (e) 800°C, and (f) 900°C.

nature of sorbate ions on the morphology of the sample. Presumably, the adsorption of excess anions occurs continuously while the precipitate is formed. In particular, this is confirmed by thermogravimetry. At the same time, equilibrium anion sorption via processes like

$$\equiv Zr\text{–}O\text{–}H(solid) + H^+(sln) + NO_3^-(sln) = \equiv Zr\text{–}NO_3^-(solid) + H_2O(sln) \quad (1)$$

at high pHs does not lead to a considerable difference in the bulk and surface properties of the precipitate. However, removal of some protons of ≡Zr–O–H groups from the surface at high pHs, which is not fully balanced by the adsorption of bulky ammonium ions in their place, can endow particles with a negative charge; this charge, because of the electrostatic repulsion of similarly charged surfaces, keeps them from aggregating.

Micrographs of samples calcined at 100°C verify this suggestion. All samples prepared at pH ≤ 6 are represented by bulky aggregations with smooth surfaces. Destruction products can be found only in some regions in the form of elongated platelets (Fig. 6a). Samples prepared at high pHs have highly developed surfaces; they consist of small rounded particles with sizes of about 40–50 nm (Fig. 6b). The mean particle size of zirconium hydroxide calculated from X-ray powder diffraction data (Fig. 5) and surface area measurements is also close to 50 nm.

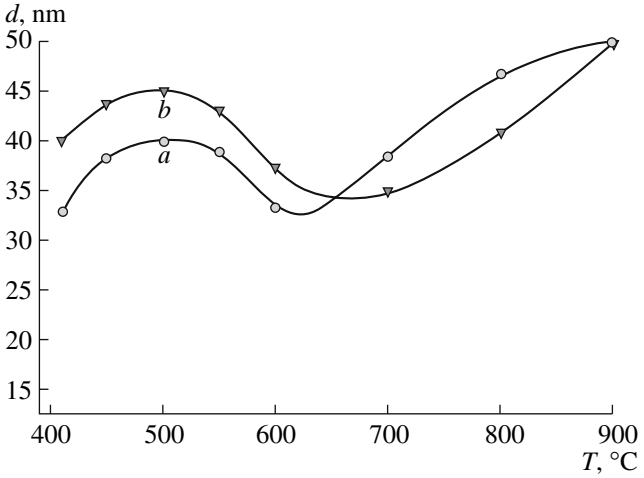

Fig. 5. Crystal size vs. treatment temperature for hydrous zirconium dioxide samples prepared at pH equal to (a) 4 and (b) 9.

An increase in the treatment temperature to 350°C (above the first exotherm) leads to a relatively small decrease of the surface area in the samples precipitated from alkaline solutions. As a result, particles slightly decrease in sizes and become more uniform (Fig. 6c).

After structure formation at 550°C, the surface area of crystalline ZrO_2 decreases to 20 m^2/g. Two types of particles are clearly seen in micrographs: anisotropic particles 30 × (100–150) nm and rounded particles with an average size of 37–38 nm (pH 4) and 48 nm (pH 9).

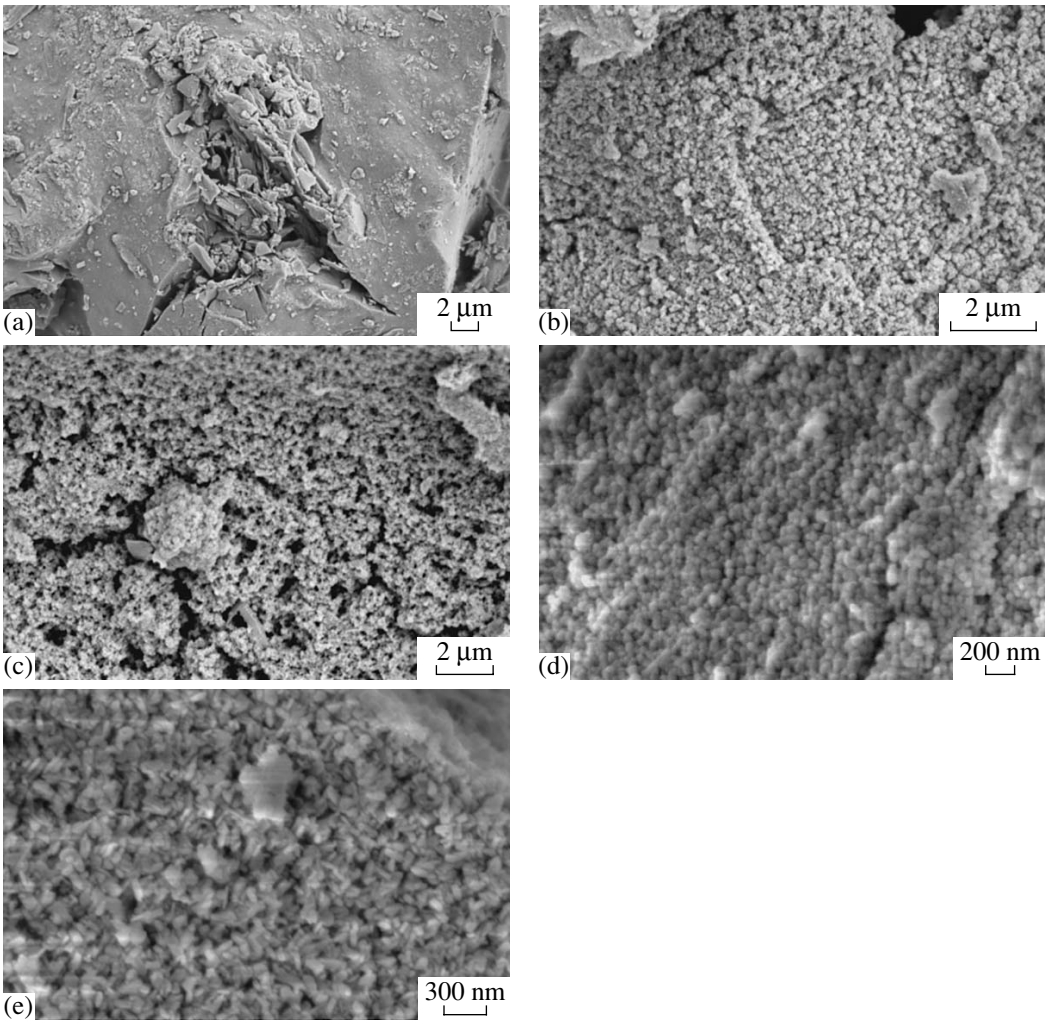

Fig. 6. Electron micrographs for hydrous zirconium dioxide samples prepared at pH equal to (a, d, e) 4 and (b, c) 9 and calcined at (a, b) 100°C, (c) 350°C, and (d, e) 550°C.

Probably, the anisotropic particles are aggregates of several crystals and the isotropic ones are individual crystals, whose sizes are close to the coherence lengths of the samples. Both types of particles are observable for samples precipitated at either low or high pHs (Figs. 6d, 6e).

The above data supplement the interpretation of thermolysis processes. The adsorption of excess nitrate ions on samples prepared at high pHs stabilizes the nanoparticles of hydrous zirconium dioxide, as mentioned above. The developed surface precludes the formation of an ordered structure of oxide; as a result, the aggregation and crystallization temperatures of monoclinic ZrO_2 increase. At elevated temperatures, however, the excess energy accumulated in nanoparticles of hydrous zirconium dioxide induces crystallization with great heat evolution. The same is enhanced by the dramatic decrease in the surface area of particles, accompanied by an extra heat evolution on account of the decreased effect of surface tension.

Specific surface areas for selected hydrous zirconium dioxide samples after various heat treatments

Precursor	Precipitation pH	Treatment temperature, °C	Specific surface area, m^2/g
$ZrO(NO_3)_2$	4	100	1–2*
$ZrO(NO_3)_2$	4	550	20
$ZrO(NO_3)_2$	6	100	1–2*
$ZrO(NO_3)_2$	7	100	203
$ZrO(NO_3)_2$	9	100	199
$ZrO(NO_3)_2$	9	350	173
$ZrO(NO_3)_2$	9	550	17

* For these samples, the specific surface area is comparable to its determination error; for the others, the determination error is ±10%.

ACKNOWLEDGMENTS

The authors are grateful for financial support from the federal program "Study and Development of the Priorities of the Science and Engineering Complex of Russia in 2007–2012" and the program "Theoretical and Experimental Study of the Nature of Chemical Bonds on the Mechanisms of the Most Important Chemical Reactions and Processes" of the Chemistry and Materials Science Department of the Russian Academy of Sciences.

REFERENCES

1. T. N. Perekhozhaeva and L. M. Sharygin, Kolloid. Zh. **51** (5), 930 (1989).
2. D. Ward and E. Ko, Chem. Mater **5,** 956 (1993).
3. L. G. Karakchiev and N. Z. Lyakhov, Neorg. Mater. **34** (5), 575 (1998).
4. A. A. Burukhin, N. N. Oleinikov, B. R. Churagulov, et al., Vestn. Voronezhsk. Gos. Tekhn. Univ., Ser. Materialoved., No. 1.5, 19 (1999).
5. J. Nawrocki, P. W. Carr, M. J. Annen, and S. Froelicher, Anal. Chim. Acta **327**, 261 (1996).
6. A. Cliearfield, *Inorganic Ion Exchange Materials* (CRC, Boca Raton FL, 1982).
7. A. B. Yaroslavtsev, Usp. Khim. **66** (7), 641 (1997).
8. V. A. Tarnopolsky, A. D. Aliev, B. R. Churagulov, et al., Solid State Ionics **162–163**, 225 (2003).
9. E. Yu. Voropaeva, I. A. Stenina, and A. B. Yaroslavtsev, Zh. Neorg. Khim. **47** (1), 5 (2007).
10. A. V. Erin, Z. N. Prozorovskaya, and A. B. Yaroslavtsev, Zh. Neorg. Khim. **38** (2), 200 (1993).
11. A. L. Klyachko-Gurvich, Izv. Akad. Nauk SSSR, Ser. Khim., No. 10, 1884 (1961).
12. C. B. Amphlett, *Inorganic Ion Exchangers* (Elsevier, Amsterdam/London/New York, 1964).